**NOTE: THE FIGURES IN THIS SECTION ARE INTENDED TO SHOW THE REPRESENTATIVE DATA.
THEY ARE NOT MEANT TO BE COMPLETE COMPILATIONS OF ALL THE WORLD'S RELIABLE DATA.**

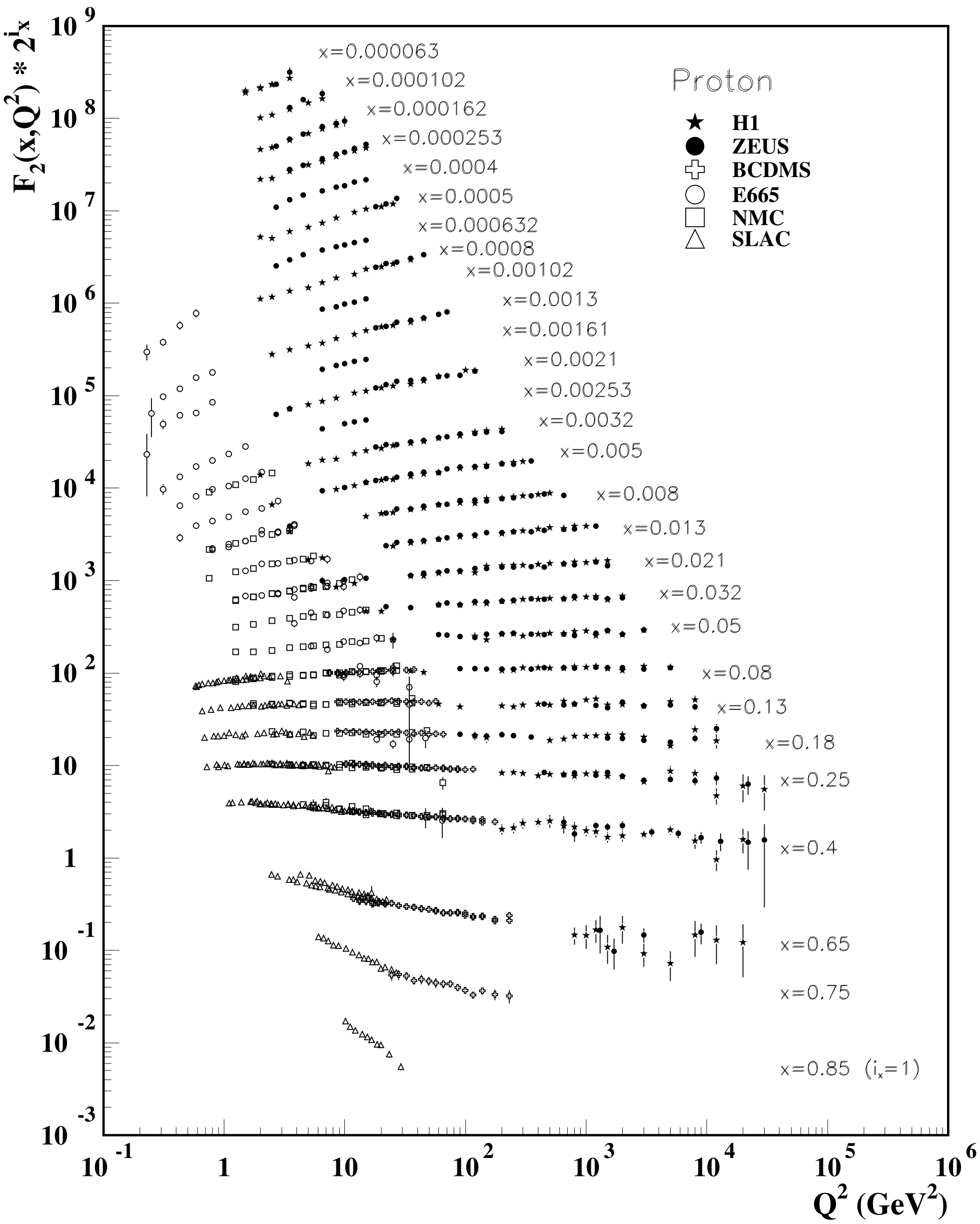


**Figure 16.7:** The proton structure function $F_2^p$ measured in electromagnetic scattering of positrons on protons (collider experiments ZEUS and H1), in the kinematic domain of the HERA data, for $x > 0.00006$ (*cf.* Fig. 16.10 for data at smaller $x$ and $Q^2$), and for electrons (SLAC) and muons (BCDMS, E665, NMC) on a fixed target. Statistical and systematic errors added in quadrature are shown. The data are plotted as a function of $Q^2$ in bins of fixed $x$. Some points have been slightly offset in $Q^2$ for clarity. The ZEUS binning in $x$ is used in this plot; all other data are rebinned to the $x$ values of the ZEUS data. For the purpose of plotting, $F_2^p$ has been multiplied by $2^{i_x}$, where $i_x$ is the number of the $x$ bin, ranging from $i_x = 1$ ($x = 0.85$) to $i_x = 28$ ($x = 0.000063$). References: **H1**—C. Adloff *et al.*, Eur. Phys. J. **C21**, 33 (2001); C. Adloff *et al.*, Eur. Phys. J. **C30**, 1 (2003); **ZEUS**—S. Chekanov *et al.*, Eur. Phys. J. **C21**, 443 (2001); S. Chekanov *et al.*, Phys. Rev. **D70**, 052001 (2004); **BCDMS**—A.C. Benvenuti *et al.*, Phys. Lett. **B223**, 485 (1989) (as given in [56]) ; **E665**—M.R. Adams *et al.*, Phys. Rev. **D54**, 3006 (1996); **NMC**—M. Arneodo *et al.*, Nucl. Phys. **B483**, 3 (1997); **SLAC**—L.W. Whitlow *et al.*, Phys. Lett. **B282**, 475 (1992).

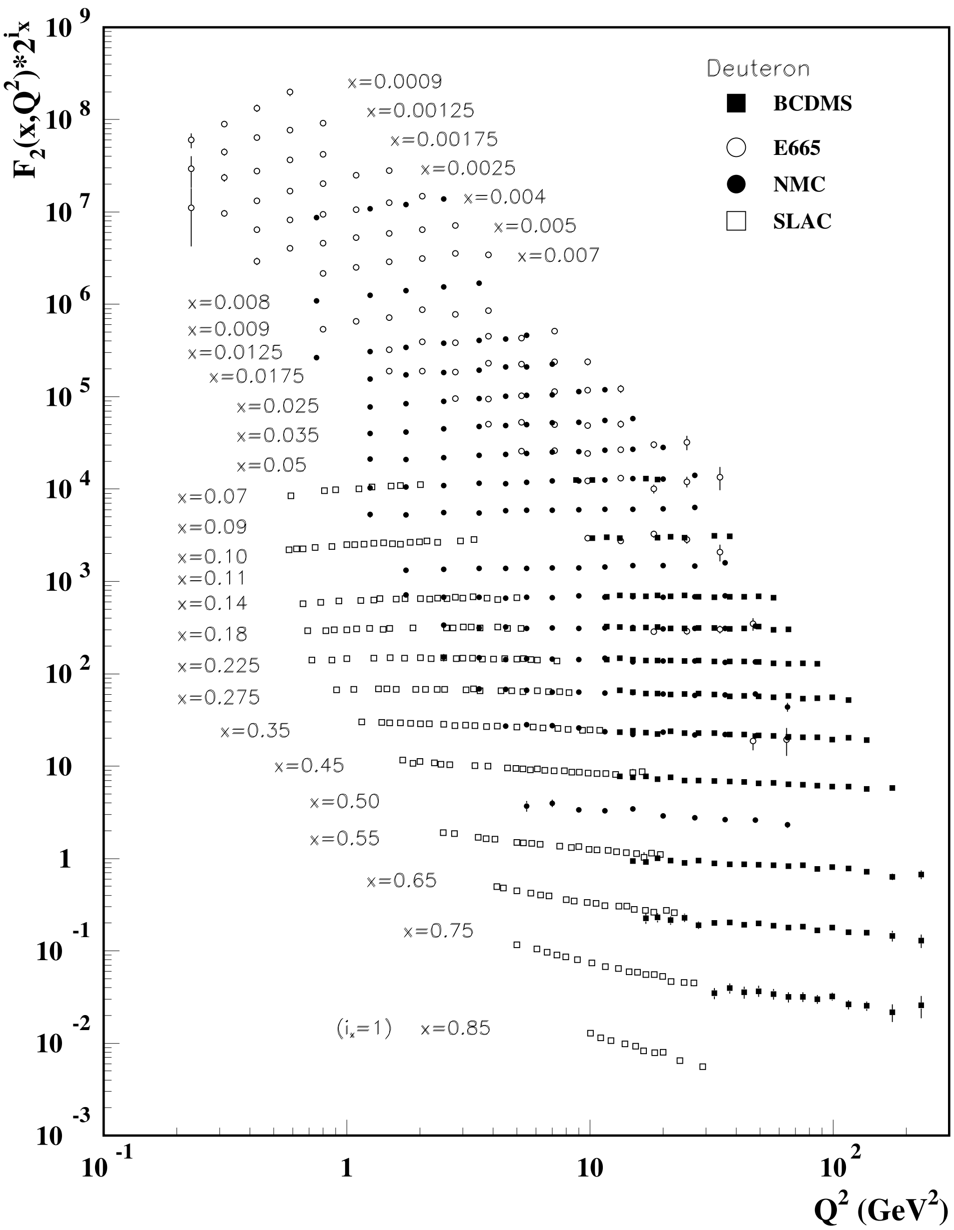


**Figure 16.8:** The deuteron structure function $F_2^d$ measured in electromagnetic scattering of electrons (SLAC) and muons (BCDMS, E665, NMC) on a fixed target, shown as a function of $Q^2$ for bins of fixed $x$. Statistical and systematic errors added in quadrature are shown. For the purpose of plotting, $F_2^d$ has been multiplied by $2^{i_x}$, where $i_x$ is the number of the $x$ bin, ranging from 1 ($x = 0.85$) to 29 ($x = 0.0009$). References: **BCDMS**—A.C. Benvenuti *et al.*, Phys. Lett. **B237**, 592 (1990). **E665, NMC, SLAC**—same references as Fig. 16.7.

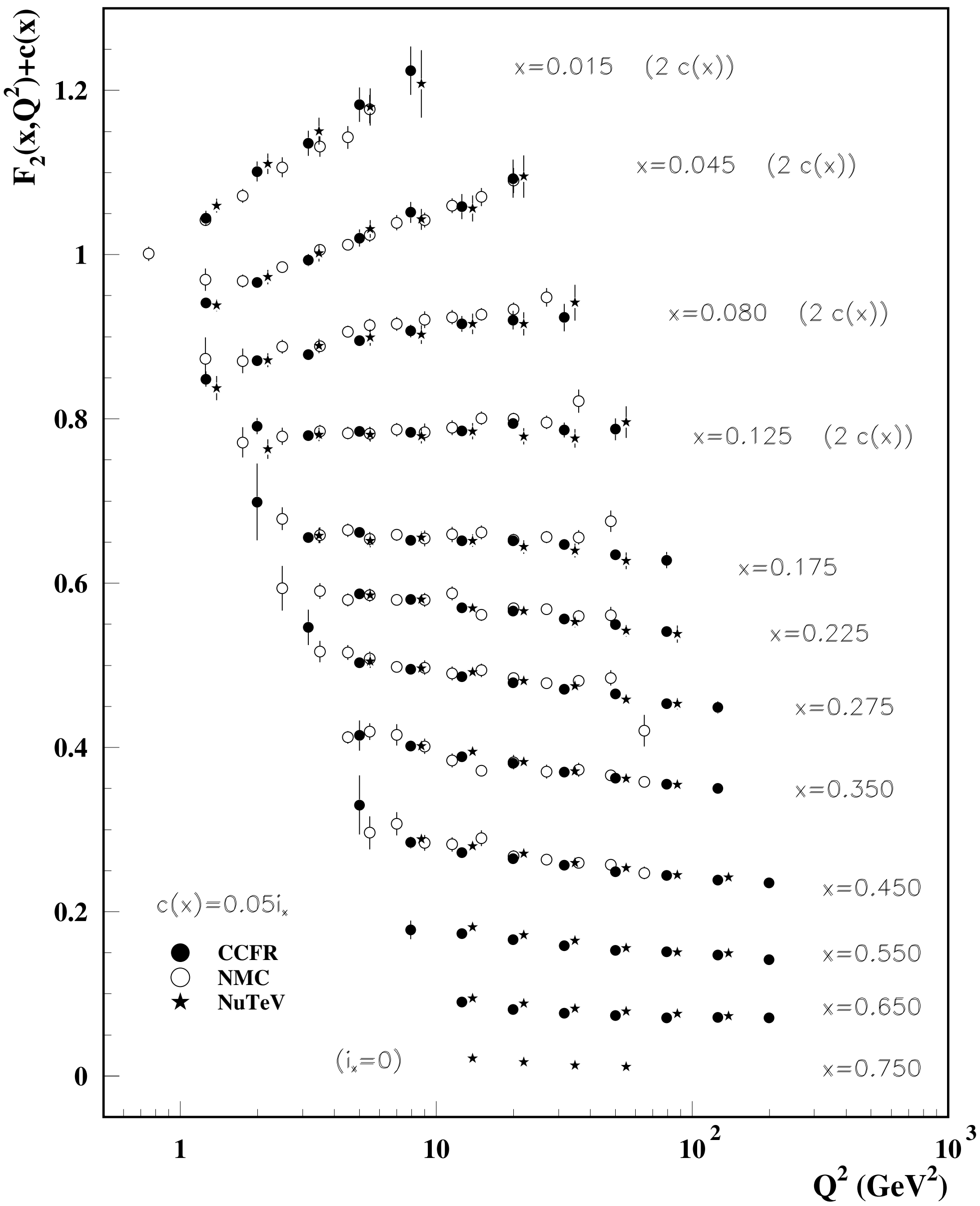


**Figure 16.9:** The deuteron structure function $F_2$ measured in deep inelastic scattering of muons on a fixed target (NMC) is compared to the structure function $F_2$ from neutrino-iron scattering (CCFR and NuTeV) using $F_2^{\mu} = (5/18)F_2^{\nu} - x(s+\overline{s})/6$, where heavy-target effects have been taken into account. The data are shown versus $Q^2$, for bins of fixed $x$. The NMC data have been rebinned to CCFR and NuTeV $x$ values. Statistical and systematic errors added in quadrature are shown. For the purpose of plotting, a constant $c(x) = 0.05 i_x$ is added to $F_2$, where $i_x$ is the number of the $x$ bin, ranging from 0 ($x = 0.75$) to 7 ($x = 0.175$). For $i_x = 8$ ($x = 0.125$) to 11 ($x = 0.015$), $2c(x)$ has been added. References: **NMC**—M. Arneodo *et al.*, Nucl. Phys. **B483**, 3 (1997); **CCFR/NuTeV**—U.K. Yang *et al.*, Phys. Rev. Lett. **86**, 2741 (2001); **NuTeV**—M. Tzanov *et al.*, Phys. Rev. **D74**, 012008 (2006).

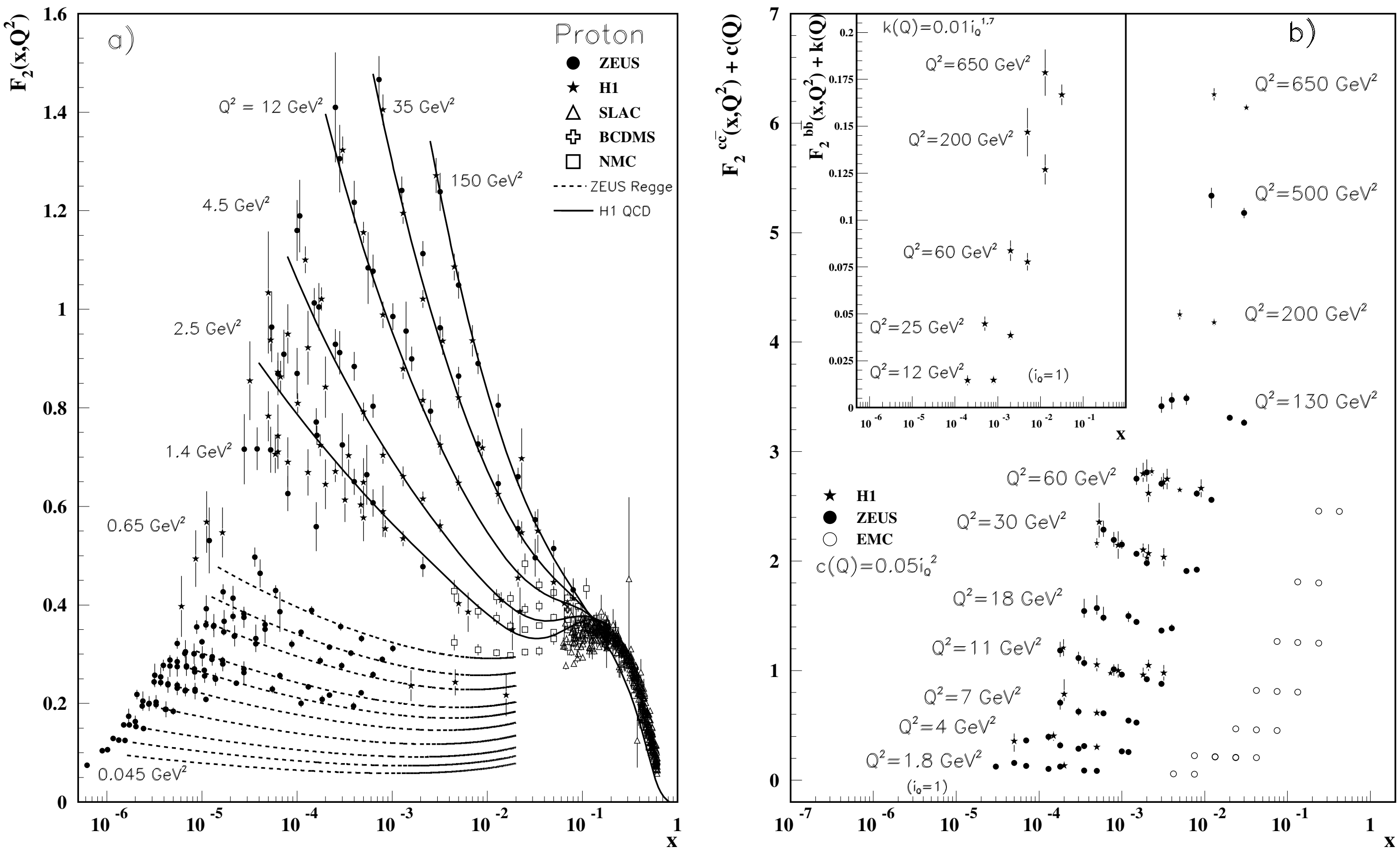


**Figure 16.10:** a) The proton structure function $F_2^p$ mostly at small $x$ and $Q^2$, measured in electromagnetic scattering of positrons (H1, ZEUS), electrons (SLAC), and muons (BCDMS, NMC) on protons. Lines are ZEUS and H1 parameterizations for lower (Regge) and higher (QCD) $Q^2$. The width of the bins can be up to 10% of the stated $Q^2$. Some points have been slightly offset in $x$ for clarity. References: **ZEUS**—J. Breitweg *et al.*, Phys. Lett. **B407**, 432 (1997); J. Breitweg *et al.*, Eur. Phys. J. **C7**, 609 (1999); J. Breitweg *et al.*, Phys. Lett. **B487**, 53 (2000) (both data and ZEUS Regge parameterization); S. Chekanov *et al.*, Eur. Phys. J. **C21**, 443 (2001); S. Chekanov *et al.*, Phys. Rev. **D70**, 052001 (2004); **H1**—C. Adloff *et al.*, Nucl. Phys. **B497**, 3 (1997); C. Adloff *et al.*, Eur. Phys. J. **C21**, 33 (2001) (both data and H1 QCD parameterization); C. Adloff *et al.*, Eur. Phys. J. **C30**, 1 (2003); A. Aktas *et al.*, Phys. Lett. **B598**, 159 (2004); **BCDMS, NMC, SLAC**—same references as Fig. 16.7.

b) The charm structure function $F_2^{c\bar{c}}(x)$, i.e. that part of the inclusive structure function $F_2^p$ arising from the production of charm quarks, measured in electromagnetic scattering of positrons on protons (H1, ZEUS) and muons on iron (EMC). The H1 points have been slightly offset in $x$ for clarity. For the purpose of plotting, a constant $c(Q) = 0.05 i_Q^2$ is added to $F_2^{c\bar{c}}$ where $i_Q$ is the number of the $Q^2$ bin, ranging from 1 ($Q^2 = 1.8$ GeV$^2$) to 11 ($Q^2 = 650$ GeV$^2$). References: **ZEUS**—J. Breitweg *et al.*, Eur. Phys. J. **C12**, 35 (2000); S. Chekanov *et al.*, Phys. Rev. **D69**, 012004 (2004); **H1**—C. Adloff *et al.*, Z. Phys. **C72**, 593 (1996); C. Adloff *et al.*, Phys. Lett. **B528**, 199 (2002); A. Aktas *et al.*, Eur. Phys. J. **C40**, 349 (2005); A. Aktas *et al.*, Eur. Phys. J. **C45**, 23 (2006); **EMC**—J.J. Aubert *et al.*, Nucl. Phys. **B213**, 31 (1983).

Inset: The bottom quark structure function $F_2^{b\bar{b}}(x)$. For the purpose of plotting, a constant $k(Q) = 0.01 i_Q^{1.7}$ is added to $F_2^{b\bar{b}}$ where $i_Q$ is the number of the $Q^2$ bin, ranging from 1 ($Q^2 = 12$ GeV$^2$) to 5 ($Q^2 = 650$ GeV$^2$). References: **H1**—A. Aktas *et al.*, Eur. Phys. J. **C40**, 349 (2005); A. Aktas *et al.*, Eur. Phys. J. **C45**, 23 (2006).

Statistical and systematic errors added in quadrature are shown for both plots. The data are given as a function of $x$ in bins of $Q^2$.

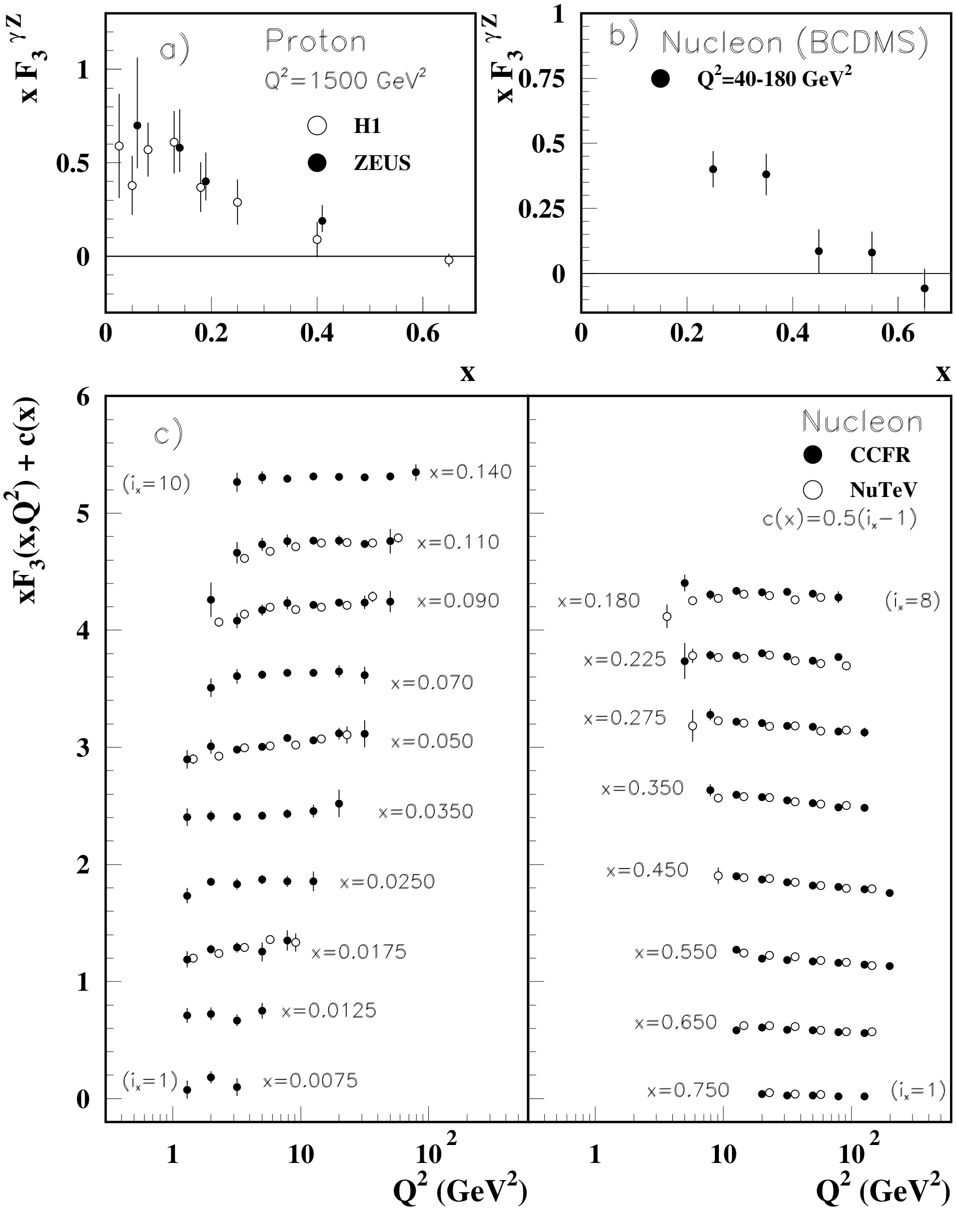


**Figure 16.11:** The structure function $xF_3^{\gamma Z}$ measured in electroweak scattering of **a)** electrons on protons (H1 and ZEUS) and **b)** muons on carbon (BCDMS). The ZEUS points have been slightly offset in $x$ for clarity. References: **H1**—C. Adloff *et al.*, Eur. Phys. J. **C30**, 1 (2003); **ZEUS**—S. Chekanov *et al.*, Eur. Phys. J. **C28**, 175 (2003); **BCDMS**—A. Argento *et al.*, Phys. Lett. **B140**, 142 (1984).
**c)** The structure function $xF_3$ of the nucleon measured in $\nu$-Fe scattering. The data are plotted as a function of $Q^2$ in bins of fixed $x$. For the purpose of plotting, a constant $c(x) = 0.5(i_x - 1)$ is added to $xF_3$, where $i_x$ is the number of the $x$ bin as shown in the plot. The NuTeV points have been shifted to the nearest corresponding $x$ bin as given in the plot and slightly offset in $Q^2$ for clarity. References: **CCFR**—W.G. Seligman *et al.*, Phys. Rev. Lett. **79**, 1213 (1997). **NuTeV**—M. Tzanov *et al.*, Phys. Rev. **D74**, 012008 (2006).

Statistical and systematic errors added in quadrature are shown for all plots.

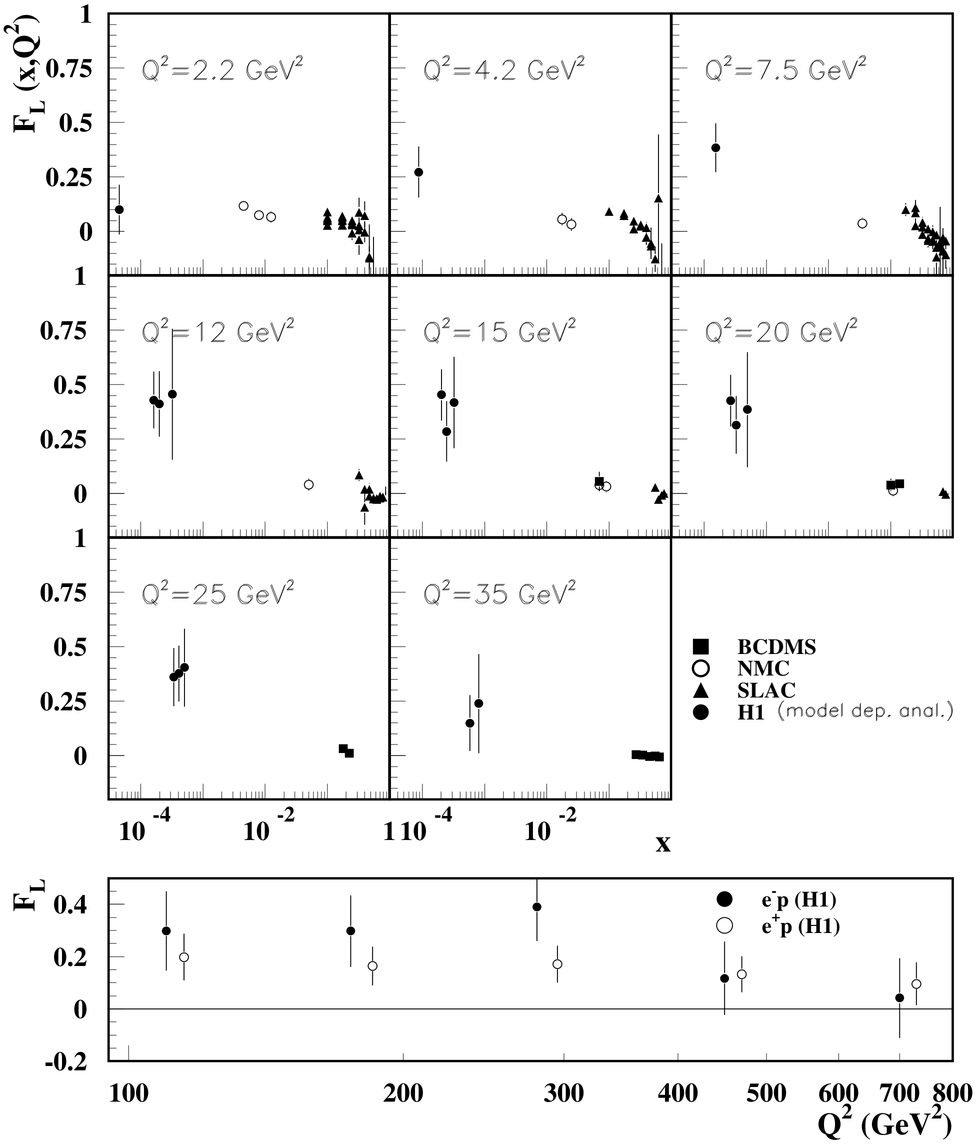


**Figure 16.12:** Top panel: The longitudinal structure function $F_L$ as a function of $x$ in bins of fixed $Q^2$ measured on the proton (except for the SLAC data which also contain deuterium data). BCDMS, NMC, and SLAC results are from measurements of $R$ (the ratio of longitudinal to transverse photon absorption cross sections) which are converted to $F_L$ by using the BDCMS parameterization of $F_2$ (A.C. Benvenuti *et al.*, Phys. Lett. **B223**, 485 (1989)). It is assumed that the $Q^2$ dependence of the fixed-target data is small within a given $Q^2$ bin. References: **H1**—C. Adloff *et al.*, Eur. Phys. J. **C21**, 33 (2001); **BCDMS**—A. Benvenuti *et al.*, Phys. Lett. **B223**, 485 (1989); **NMC**—M. Arneodo *et al.*, Nucl. Phys. **B483**, 3 (1997); **SLAC**—L.W. Whitlow *et al.*, Phys. Lett. **B250**, 193 (1990) and numerical values from the thesis of L.W. Whitlow (SLAC-357).

Bottom panel: Higher $Q^2$ values of the longitudinal structure function $F_L$ as a function of $Q^2$ given at the measured $x$ for $e^+/e^-$-proton scattering. Points have been slightly offset in $Q^2$ for clarity. References: **H1**—C. Adloff *et al.*, Eur. Phys. J. **C30**, 1 (2003).

The H1 results shown in both plots require the assumption of the validity of the QCD form for the $F_2$ structure function in order to extract $F_L$. Statistical and systematic errors added in quadrature are shown for both plots.

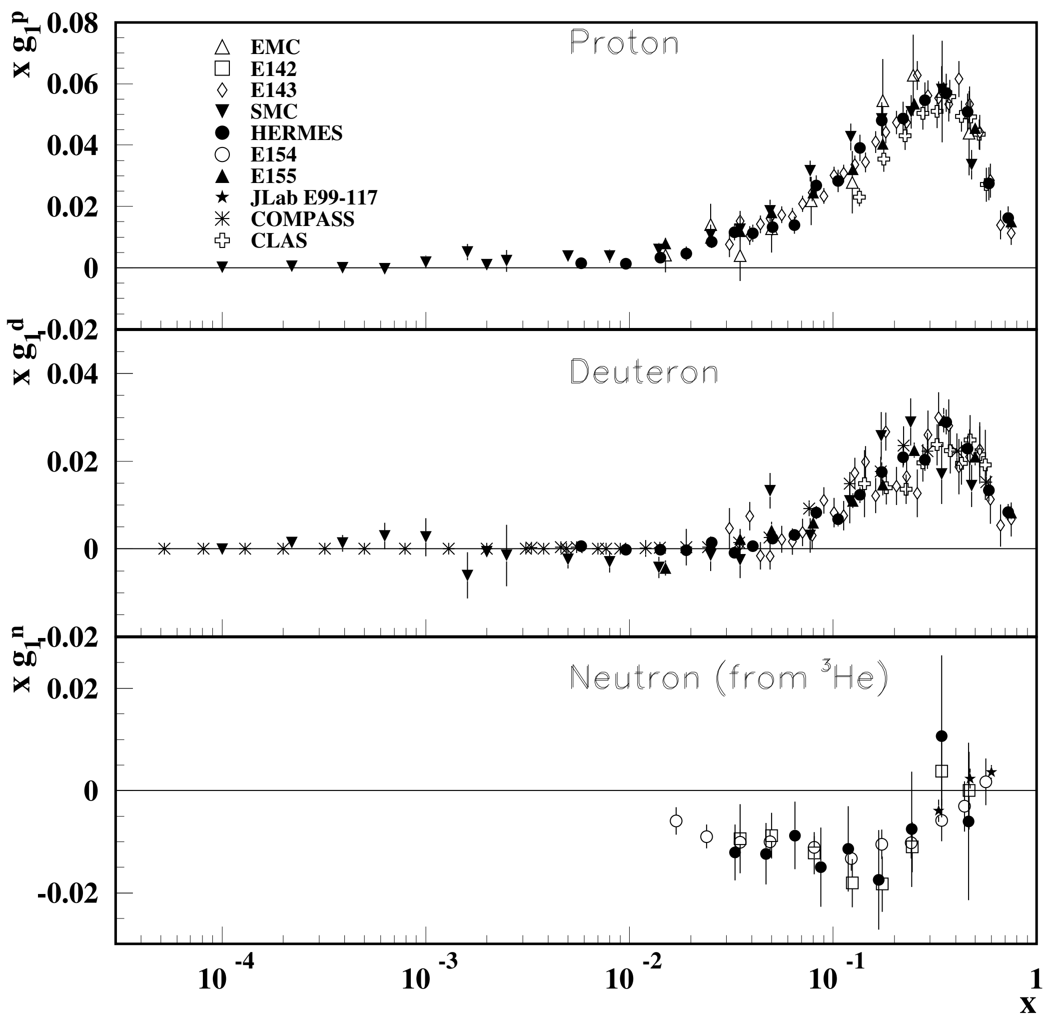


**Figure 16.13:** The spin-dependent structure function $xg_1(x)$ of the proton, deuteron, and neutron (from $^3$He target) measured in deep inelastic scattering of polarized electrons/positrons: E142 ($Q^2 \sim 0.3-10$ GeV$^2$), E143 ($Q^2 \sim 0.3-10$ GeV$^2$), E154 ($Q^2 \sim 1-17$ GeV$^2$), E155 ($Q^2 \sim 1-40$ GeV$^2$), JLab E99-117 ($Q^2 \sim 2.71-4.83$ GeV$^2$), HERMES ($Q^2 \sim 0.18-20$ GeV$^2$), CLAS ($Q^2 \sim 1-5$ GeV$^2$) and muons: EMC ($Q^2 \sim 1.5-100$ GeV$^2$), SMC ($Q^2 \sim 0.01-100$ GeV$^2$), COMPASS ($Q^2 \sim 0.001-100$ GeV$^2$), shown at the measured $Q^2$ (except for EMC data given at $Q^2 = 10.7$ GeV$^2$ and E155 data given at $Q^2 = 5$ GeV$^2$). Note that $g_1^n(x)$ may also be extracted by taking the difference between $g_1^d(x)$ and $g_1^p(x)$, but these values have been omitted in the bottom plot for clarity. Statistical and systematic errors added in quadrature are shown. References: **EMC**—J. Ashman *et al.*, Nucl. Phys. **B328**, 1 (1989); **E142**—P.L. Anthony *et al.*, Phys. Rev. **D54**, 6620 (1996); **E143**—K. Abe *et al.*, Phys. Rev. **D58**, 112003 (1998); **SMC**—B. Adeva *et al.*, Phys. Rev. **D58**, 112001 (1998), B. Adeva *et al.*, Phys. Rev. **D60**, 072004 (1999) and Erratum-Phys. Rev. **D62**, 079902 (2000); **HERMES**—A. Airapetian *et al.*, Phys. Rev. **D75**, 012007 (2007) and K. Ackerstaff *et al.*, Phys. Lett. **B404**, 383 (1997); **E154**—K. Abe *et al.*, Phys. Rev. Lett. **79**, 26 (1997); **E155**—P.L. Anthony *et al.*, Phys. Lett. **B463**, 339 (1999) and P.L. Anthony *et al.*, Phys. Lett. **B493**, 19 (2000); **Jlab-E99-117**—X. Zheng *et al.*, Phys. Rev. **C70**, 065207 (2004); **COMPASS**—V.Yu. Alexakhin *et al.*, Phys. Lett. **B647**, 8 (2007) and E.S. Ageev *et al.*, Phys. Lett. **B647**, 330 (2007); **CLAS**—K.V. Dharmawardane *et al.*, Phys. Lett. **B641**, 11 (2006) (which also includes resonance region data not shown on this plot).

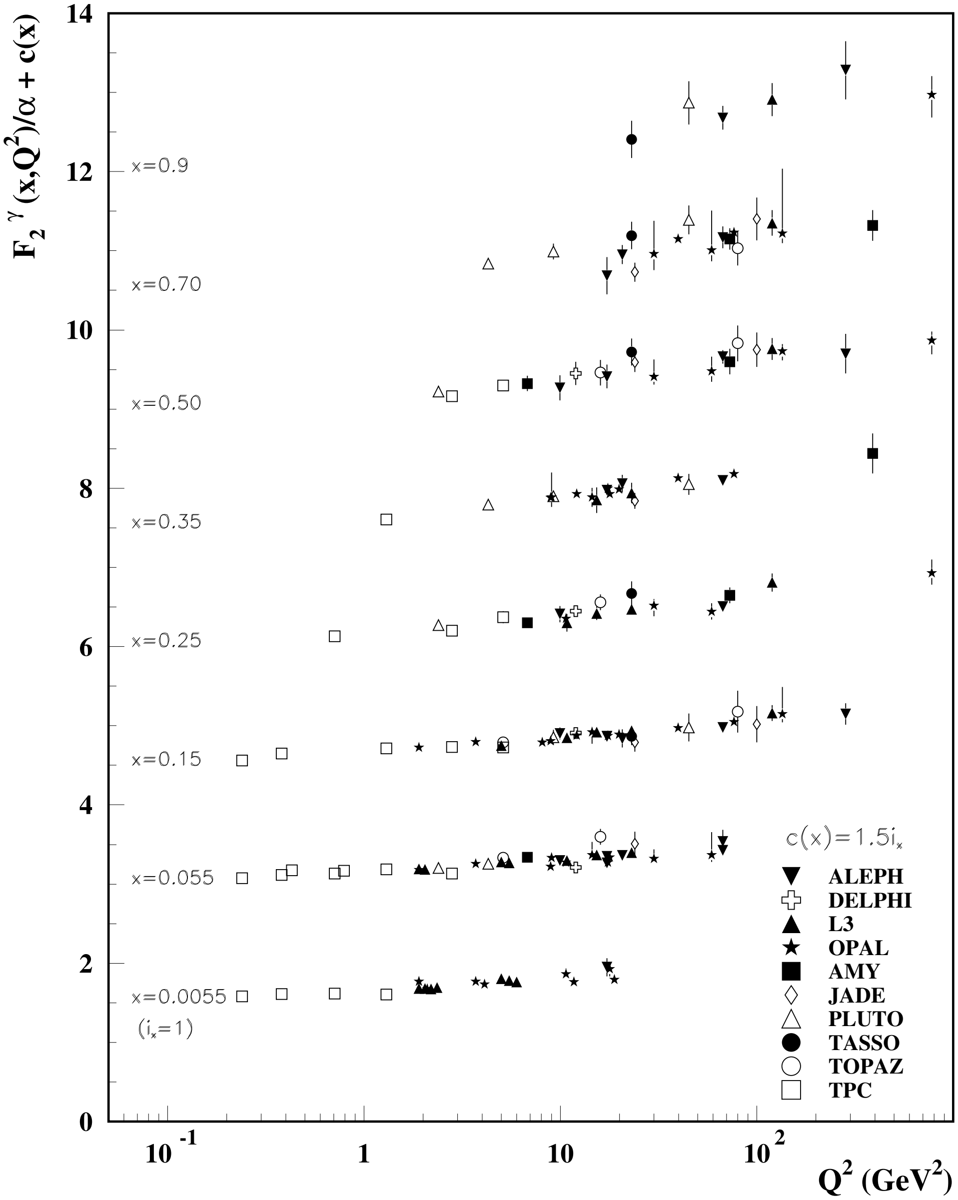


**Figure 16.14:** The hadronic structure function of the photon $F_2^{\gamma}$ divided by the fine structure constant $\alpha$ measured in $e^+e^-$ scattering, shown as a function of $Q^2$ for bins of $x$. Data points have been shifted to the nearest corresponding $x$ bin as given in the plot. Some points have been offset in $Q^2$ for clarity. Statistical and systematic errors added in quadrature are shown. For the purpose of plotting, a constant $c(x) = 1.5 i_x$ is added to $F_2^{\gamma}/\alpha$ where $i_x$ is the number of the $x$ bin, ranging from 1 ($x = 0.0055$) to 8 ($x = 0.9$). References: **ALEPH**–R. Barate *et al.*, Phys. Lett. **B458**, 152 (1999); A. Heister *et al.*, Eur. Phys. J. **C30**, 145 (2003);**DELPHI**–P. Abreu *et al.*, Z. Phys. **C69**, 223 (1995); **L3**–M. Acciarri *et al.*, Phys. Lett. **B436**, 403 (1998); M. Acciarri *et al.*, Phys. Lett. **B447**, 147 (1999); M. Acciarri *et al.*, Phys. Lett. **B483**, 373 (2000); **OPAL**–A. Ackerstaff *et al.*, Phys. Lett. **B411**, 387 (1997); A. Ackerstaff *et al.*, Z. Phys. **C74**, 33 (1997); G. Abbiendi *et al.*, Eur. Phys. J. **C18**, 15 (2000); G. Abbiendi *et al.*, Phys. Lett. **B533**, 207 (2002) (note that there is overlap of the data samples in these last two papers); **AMY**–S.K. Sahu *et al.*, Phys. Lett. **B346**, 208 (1995); T. Kojima *et al.*, Phys. Lett. **B400**, 395 (1997); **JADE**–W. Bartel *et al.*, Z. Phys. **C24**, 231 (1984); **PLUTO**–C. Berger *et al.*, Phys. Lett. **142B**, 111 (1984); C. Berger *et al.*, Nucl. Phys. **B281**, 365 (1987); **TASSO**–M. Althoff *et al.*, Z. Phys. **C31**, 527 (1986); **TOPAZ**–K. Muramatsu *et al.*, Phys. Lett. **B332**, 477 (1994); **TPC/Two Gamma**–H. Aihara *et al.*, Z. Phys. **C34**, 1 (1987).